

Repair of Large Articular Osteochondral Defects Using Hybrid Scaffolds and Bone Marrow-Derived Mesenchymal Stem Cells in a Rabbit Model

XINXIN SHAO, M.D., Ph.D.,¹ JAMES C.H. GOH, Ph.D.,^{1,2}
DIETMAR W. HUTMACHER, Ph.D., M.B.A.,^{1,2}
ENG HIN LEE, M.D.¹, and GE ZIGANG, Ph.D.¹

ABSTRACT

In order to evaluate the repair potential in large osteochondral defects on high load-bearing sites, a hybrid scaffold system was made of three-dimensional porous Polycaprolactone (PCL) scaffold for the cartilage and tricalcium phosphate–reinforced PCL for the bone portion. Osteochondral defects of 4-mm diameter \times 5.5-mm depth were created in the medial femoral condyle of adult New Zealand White rabbits. The defects were treated with hybrid scaffolds without cells (control group) or seeded with allogenic bone marrow–derived mesenchymal stem cells (BMSC) in each part (experimental group) by press-fit implantation. Implanted cells were tracked using Adeno-LacZ labeling. Repair tissues were evaluated at 3 and 6 months after implantation. Overall, the experimental group showed superior repair results as compared to the control group using gross examination, qualitative and quantitative histology, and biomechanical assessment. With BMSC implantation, the hybrid scaffolds provided sufficient support to new osteochondral tissues formation. The bone regeneration was consistently good from 3 to 6 months with firm integration to the host tissue. Cartilage layer resurfacing was more complicated. All of the samples showed cartilage tissues mixed with PCL scaffold filaments at 3 months. Histology at 6 months revealed some degradation phenomenon in several samples whereas others had a good appearance; however, the Young's moduli from the experimental group (0.72 MPa) approached that of normal cartilage (0.81 MPa). *In vivo* viability of implanted cells was demonstrated by the retention for 6 weeks in the scaffolds. This investigation showed that PCL-based hybrid scaffolds with BMSC may be an alternative treatment for large osteochondral defects in high-loading sites.

INTRODUCTION

OSTEochondral defect repair is a challenging problem in the field of orthopedic surgery, because the mature articular cartilage is an avascular tissue that has limited capacity for self-repair. Particularly for large osteochondral injuries, mechanical instability and insuffi-

cient migration of bone marrow cells usually results in functionally poor fibrous repair tissue in the loaded joint environment.^{1,2} Various approaches have been investigated to improve the healing of osteochondral injuries, including periosteal or perichondrial resurfacing, and chondrocyte or bone marrow–derived mesenchymal cells transplantation.^{3–5} These different graft implantations

¹Department of Orthopaedic Surgery, National University of Singapore.

²Division of Bioengineering, National University of Singapore.

have not produced consistent and reproducible successes. The repair tissues have limited durability and show degenerative changes after long-term follow-up.⁶

Tissue engineering principles that combined living cells with scaffolds are promising techniques for osteochondral defect repair and articular resurfacing.^{7,8} The scaffold is one of the major components in these tissue engineering strategies. To date, biological or synthetic scaffolds combined with chondrocytes or mesenchymal cells have been widely used in osteochondral defect repair experiments.^{9–11} However, most of these methods have focused on the use of a single material, for instance, collagen,^{4,9} alginate,¹⁰ hydroxyapatite,¹¹ or synthesized polymers,^{6,11} with homogeneous biological and mechanical properties as an osteochondral scaffold. In reality, the articular osteochondral injury involves damage to both bone and cartilage. These tissues have different intrinsic structures, although they are well integrated to each other for weight-bearing and functional joint movement. Tissue engineering techniques should mimic this physiological structure. Therefore, fabricating the composite scaffolds with layers of different materials that can benefit both bone and cartilage regeneration is potentially a better technique for osteochondral repair.

Currently, a few hybrids or biphased scaffolds have been studied in *in vivo* experimental models. Gao *et al.*¹² reported their study on the use of hybrid scaffolds implanted subcutaneously in a rat model. Rat bone marrow mesenchymal cells were loaded in a hyaluronan sponge for cartilage and in calcium phosphate ceramic for bone; fibrocartilage tissue formation was observed in the sponge and bone was detected in the ceramic portion after 6 weeks' implantation. Frenkel *et al.*¹³ used a two-layered collagen matrix consisting of a dense collagen layer as subchondral support and a porous upper matrix to support seeded chondrocytes. This bilayer implant allowed sustained hyaline-like cartilage repair of articular defects during the entire 6-month period in a rabbit model. Another study by van Susante *et al.*¹⁴ reported an investigation in which chondrocytes were seeded into fibrin glue and then placed upon hydroxyapatite cylinders, but this failed to produce a stable osteochondral base and resulted in overlaying fibrocartilage tissue formation. Overall, few studies have indicated that a hybrid scaffold system could be a feasible approach for osteochondral repair; however, a suitable combination of biomaterials and sufficient *in vivo* experiments still need to be selected and investigated.

In the present study, we tested the hypothesis that a hybrid scaffold system (*i.e.*, a "cartilage" layer and a "bone" layer) could provide sufficient mechanical support and improve the repair of large osteochondral defects in a rabbit model. In this hybrid scaffold system, a fully interconnected porous Polycaprolactone (PCL) scaffold was used as the "cartilage" scaffold, which was

fabricated by using a computer-controlled extrusion and deposition process—Fused Deposition Modeling (FDM). A detailed introduction into FDM was shown elsewhere.¹¹ PCL is a semicrystalline, bioresorbable polymer with stable structure and reduced sensitivity to environmental conditions. Many *in vitro* and *in vivo* biocompatibility studies have been performed, resulting in U.S. Food and Drug Administration approval of medical drug delivery devices.^{15,16} Using the FDM method, our group can fabricate highly reproducible PCL scaffolds with a honeycomb-like pattern, fully interconnected channel network, controllable porosity, and harder stiffness as comparable to cartilage or bone.¹⁵ Previous studies have shown that the PCL scaffold can provide a suitable template for cell transplantation and is capable of recruiting mesenchymal cells *in vivo* for chondrogenesis.^{17,18} For the bone portion, a tricalcium phosphate (TCP) reinforced PCL scaffold was used. Commercialized TCP is synthesized by sintering precipitated calcium-deficient apatite with Ca to P molar ratio of 1.5,¹⁹ which is a biomaterial similar to bone mineral constitution with good biocompatibility and osteoconductivity.^{19,20} TCP has been widely used as a bone substitute or as coatings on metal implants in orthopedic and dental applications to accelerate bone reconstruction or skeletal fixation.²¹ However, because of the relatively poor mechanical properties, TCP is not suitable for load-bearing sites or large bony defects. Incorporation of TCP into a polymer matrix would overcome this shortcoming. Previous studies have shown the feasibility and advantages of this composition for bone regeneration.^{11,22} Additionally, in our former study, customized PCL scaffolds were successfully used in calvarial bone defect repair.²³

Live cell implantation is another key component in tissue engineering strategies. Bone marrow-derived mesenchymal stem cells (BMSC) have been considered as promising candidates because of their rapid proliferation abilities, multiple differentiation potential, and easy harvest without additional operations. Extensive *in vitro* and *in vivo* studies have shown that BMSC can differentiate into osteoblasts or chondrocytes when placed under different inductive conditions.^{24–27} BMSC embedded in collagen gel,⁵ hyaluronic acid-based adhesive glue,²⁸ or combined with some polymeric scaffolds²² had been widely applied to improve the full-thickness cartilage injury repair in rabbit⁵ and goat model.²⁸ BMSC from rat,²⁹ rabbit,³⁰ and canine³¹ have also been used in the studies related to osteogenesis and segmental bone defect healing. Therefore, BMSC were used in the current study for the promotion of osteochondral repair.

The objective of this study was to investigate the application of a hybrid scaffold system (PCL-TCP as bone scaffold and PCL as cartilage matrix) loaded with BMSC in the repair of large osteochondral defects in a rabbit model.

MATERIALS AND METHODS

Scaffold fabrication

The PCL and PCL-TCP scaffolds were fabricated using the FDM technique as previously described.^{15,17} Briefly, PCL filament was preformed with a fiber-spinning machine (Alex James & Associates Inc., Greenville, SC) from PCL pellets. As for the PCL-TCP filament, it was also preformed with the fiber-spinning machine. The composition of TCP in the PCL-TCP mixture is 20% by weight. Scaffold sheets were made from the PCL and the PCL-TCP filaments on a FDM 3000 3-D rapid prototyping system from Stratasys Inc. (Eden Prairie, MN). The scaffold morphology and pore size were studied under a scanning electron microscope. Both PCL and PCL-TCP scaffolds have a lay-down pattern of 0/60°/120° and 65% porosity. The honeycomb-like pore size fell within the range of 380 × 430 × 590 μm (Fig. 1).

Culture of BMSC

Three-month-old New Zealand White rabbits were selected for allogeneic BMSC isolation and culture. As described before,^{5,27} 4–5-mL bone marrow was aspirated from the disinfected iliac crest of rabbits by an 18-gauge cannular needle on a 10-mL syringe, containing 1 mL of heparin (Sigma, Singapore) solution (1000 U/mL). The bone marrow was transferred to a 50-mL centrifuge tube and mixed with twice the volume of phosphate buffer solution (PBS). The diluted marrow mixture was centrifuged at 1500 rpm for 5 min. After centrifugation, the supernatant containing fat tissue was discarded and the cell pellets were rinsed again in PBS, then resuspended in 10-mL complete medium consisting of low-glucose Dulbecco's Modified Eagle's Medium (DMEM-LG, Gibco) supplemented with 10% fetal bovine serum, 100

U/mL penicillin and 100 μg/mL streptomycin. The cells suspension were seeded into T-75 flasks and cultured in a 37°C and 5% CO₂ incubator. Nonadherent cells were removed from cultures after 5 days by PBS washing and fresh medium change. Adherent cells clusters grew into colony-forming fibroblast-like cells in 10 to 14 days with medium change every 3 days and were subcultured until the third passage.

Preparation of hybrid scaffold constructs

PCL and PCL-TCP scaffold sheets with dimension 40 mm × 30 mm × 2.5 mm or 40 mm × 30 mm × 3 mm (length × width × height) were fabricated separately as described above. Scaffold discs with 4-mm diameter were punched from the sheets and sterilized by soaking in 75% ethanol. Fibrin glue (TISSEEL kit, Baxter AG) was used as cell-loading carrier, consisting of two components: TISSEEL fibrinogen and thrombin. For the experimental group, confluent BMSC cells were collected and resuspended in thrombin solution. Twenty microliters of thrombin solution containing 1.5 million cells was seeded into a PCL scaffold disc (Ø 4 × 2.5 mm) by micropipette. The scaffold disc was held by a sterile forceps and turned upside-down several times during the seeding process so that the cells could be distributed throughout the scaffold. A 15-μL TISSEEL solution was then added for fibrin gel formation in the scaffold. Another 1.5 million cells were seeded into PCL-TCP disc scaffold (Ø 4 × 3 mm) with the same method. After seeding, the cell-scaffold constructs were kept in complete DMEM medium for 1 to 2 h until subsequent implantation use. For the control group, the same volume fibrinogen and thrombin solutions without cells were seeded in PCL and PCL-TCP scaffolds by micropipette.

Surgical implantation

Twenty-one skeletal mature New Zealand White rabbits (5–6 months old) weighing 3 to 3.5 kg were used in the study. Eighteen rabbits received an osteochondral defect in both knees, thus producing 36 lesions. The 36 defects were randomly allocated to control and experimental groups for histological and biomechanical evaluations (Table 1). In the experimental group, defects were treated with hybrid scaffolds loaded with fibrin glue and BMSCs. In the control group, defects were treated with hybrid scaffolds and fibrin glue only. Four defects from the experimental group were used for *in vivo* cell tracing study. Another six normal knee joints from three rabbits were used as unoperated controls in biomechanical tests. The study was conducted according to the guidelines and protocols approved by an animal utilization study committee in Singapore.

Rabbits were given an intramuscular injection of xylazine (8 mg/kg) and ketamine (40 mg/kg) followed by in-

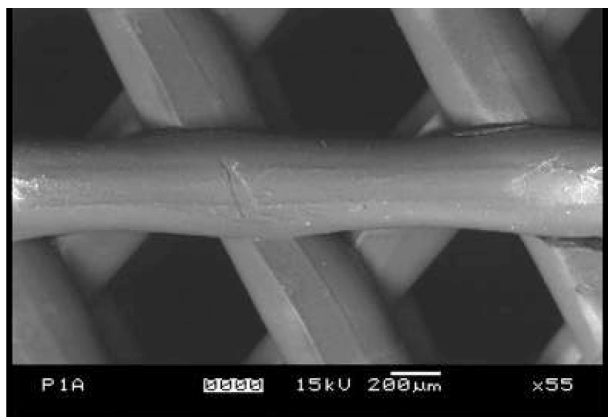


FIG. 1. SEM image of PCL scaffold showed the 0/60°/120° honeycomb-like lay-down pattern and 380 × 430 × 590-μm pore size.

TABLE 1. DISTRIBUTION OF RABBIT SAMPLES

Number of knee joints	Postoperative endpoint		
	6 week	3 month	6 month
Control	—	6	8
Experimental	4	8	10

tubation. The knee regions were then shaved and disinfected. A medial parapatellar incision was made on the knee joint. The dissection was continued until the medial femoral condyle was exposed. A 4-mm-diameter defect with 5.5-mm depth centered on the medial femoral condyle was created using a surgical drill bit (Fig. 3a). The depth of penetration was limited by a line marked on the drill bit. In the experimental group, the PCL-TCP scaffold with BMSC was implanted into the defect first as the bony portion. Then, the PCL scaffold with BMSC was pressed fit into the defect as the cartilaginous part. In the control group, the defects were treated with sequential implantation of PCL-TCP scaffold followed by the PCL scaffold without cells, but fibrinogen and thrombin was pre-loaded into these scaffolds. After implantation, the knee joint synovium, capsule, and skin were closed. The operated knee joints were allowed free movement postoperatively.

In vivo tracing of implanted cells

The E1-deleted adenoviral vector, Adeno-LacZ, containing LacZ cDNA was used as a report marker for implanted cell tracing. Briefly, the BMSCs were plated 24 h before adenoviral transduction. On the day of transduction, the cells were pre-incubated with 5 mL DMEM and then infected with Adeno-LacZ at multiplicities of infection at 800 ifu per cell for 4 h. After that, 10 mL of fresh culture medium was added to the cells and then subjected to 48 h incubation. On the third day, the infected cells were collected and seeded into PCL and PCL-TCP scaffolds as described above. The cell-scaffold constructs were implanted in the osteochondral defects using the same surgical methods described previously. The rabbits were sacrificed at 6 weeks postoperatively and the distal femora were harvested and fixed in 4% formalin overnight. Following that, the distal femur was stained in X-gal (5-bromo-4-chloro-3-indolyl-B-d-galactopyranoside) substrate 1 mg/mL, 1 mmol/L MgCl₂, 10 mmol/L K₄Fe(CN)₆, and 10 mmol/L K₃Fe(CN)₆ in PBS for 24 h. After X-gal staining, the samples were placed in 4% formalin again for complete fixation, and then the samples were decalcified and embedded in paraffin and sectioned in a coronal plane. The sections were counterstained with Safranin O.

Gross morphology and histology

At 3 and 6 months postoperatively, the rabbits were sacrificed by intravenous overdose of pentobarbital.

TABLE 2. HISTOLOGICAL SCORING SYSTEM^a

Category	Points
1 Hyaline articular cartilage, % ^b	
80–100	8
60–80	6
40–60	4
20–40	2
0–20	0
2 Surface regularity	
Smooth and intact	3
Superficial horizontal lamination	2
Fissures	2
Severe disruption, including fibrillation	0
3 Degenerative changes in repair tissue	
Severe hypercellularity	1
Mild or moderate hypercellularity	2
Normal cellularity, no cluster, normal staining	3
Normal cellularity, mild cluster, moderate staining	2
Mild or moderate hypocellularity, slight staining	1
Severe hypocellularity, poor or no staining	0
4 Structure integrity	
Normal	2
Slight disruption, including cyst	1
Severe disintegration	0
5 Cartilage thickness, % ^c	
121–150	1
81–120	2
51–80	1
0–50	0
6 Integration with adjacent cartilage, medially	
Boned	2
Partially bonded	1
No bonded	0
7 Integration with adjacent cartilage, laterally	
Boned	2
Partially bonded	1
No bonded	0
8 Bony filing of defect, % ^d	
101–125	2
76–100	3
51–75	2
26–50	1
0–25	0
9 Tidemark	
Present	1
Absent	0
10 Degenerative changes in adjacent cartilage	
Normal cellularity, no cluster, normal staining	3
Normal cellularity, mild cluster, moderate staining	2
Mild or moderate hypocellularity, slight staining	1
Severe hypocellularity, poor or no staining	0

^aBased on the system described by Solchaga *et al.*³² The score for normal osteochondral tissue is 29 points.

^bToluidine blue-stained area of repair tissue, as a percentage of total defect top area defined by defect width and adjacent normal cartilage thickness.

^cCompared with adjacent normal cartilage thickness.

^dBone formation, as a percentage of repair tissue in the defect (excluding the space occupied by scaffold).

The harvested samples were examined and photographed for evaluation. After gross examination, samples were fixed in 4% formalin, decalcified in 30% formic acid, then embedded in paraffin and cut to 8- μm -thick sections. Sections were stained with hematoxylin and eosin for the study of morphological details and with toluidine blue for cartilaginous matrix distribution. For the overall evaluation of the regenerated tissue in the defect, stained sections near the edge and center of the defect were selected and histologically scored by two individuals under blinded conditions. The osteochondral repair scale³² reported previously was modified and used in this study (Table 2). The repaired tissue was graded for hyaline cartilage formation, structure characteristics, degenerative changes, and bone filling of defect (the score for normal osteochondral tissue was 29 points). This modification was necessary because the implanted scaffold was still present and occupied space at the time of assessment. Type II collagen expression was detected by immunohistochemical analysis using a monoclonal antibody against

rabbit type II collagen (NeoMarker, Fremont, CA) and a biotin and enzyme-labeled streptavidin kit (Labvision, Fremont, CA). Briefly, the sections were pre-blocked with 3% hydrogen peroxide, and then digested with pepsin solution at 37°C for 15 min. After ultra V block, sections were incubated with Type II collagen antibody at 1:100 dilution at 37°C for 2 h. Immunohistochemical reaction was subsequently developed by the kit.

Biomechanical analysis

Indentation tests were performed on osteochondral samples using a nondestructive, *in situ* method described previously³³ by Instron 5848 micro tester machine (Canton, MA). The distal medial femoral condyles containing the area of the defect were carefully harvested and fixed in small plastic Petri dishes using polymethylmethacrylate dental cement (Meliodent, Heraeus Kulzer). The dishes were mounted on a platform that enabled alignment of the cartilage surface perpendicular to the inden-

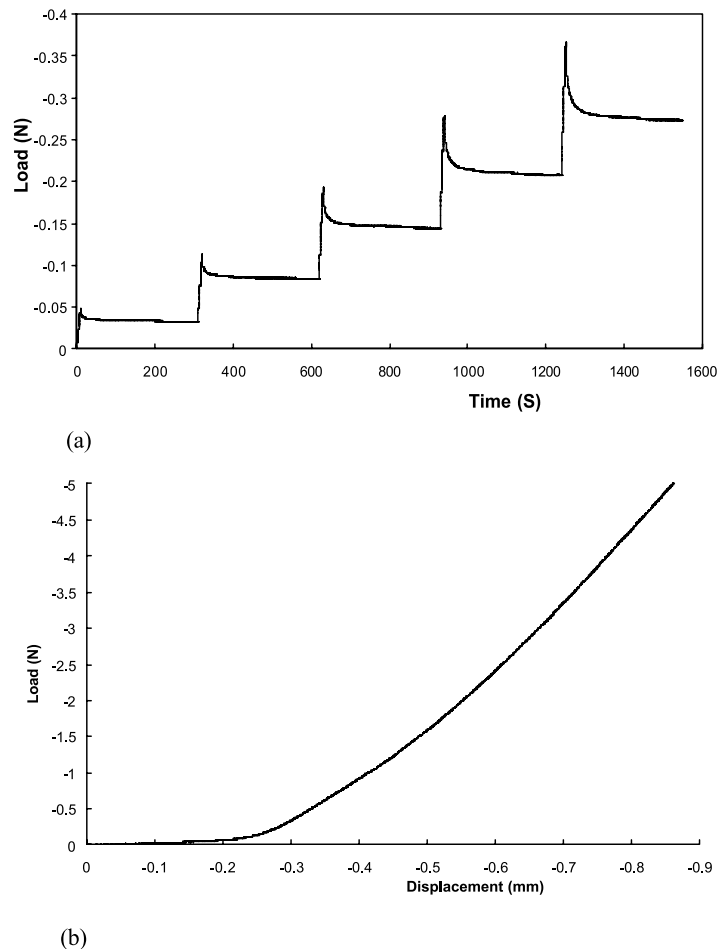


FIG. 2. (a) Typical behavior of articular cartilage during the indentation test; stepwise stress-relaxation as a function of time. (b) Cartilage thickness was determined by load versus displacement curve. Minus value in the chart denotes compression or displacement in downward direction.

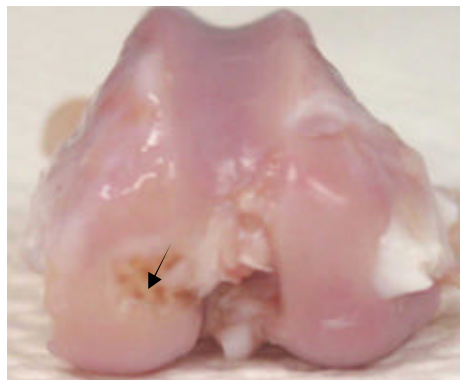
ter tip. In the test, all samples were fully submerged in physiological saline.

A 1.6-mm-diameter, porous, plane-ended indenter (Capstan Permaflow, CA) was attached to the load cell and used to probe one or two sites at the edge and center of each defect. After equilibrium to a 0.01 N tare load, indentation load was applied at five stepwise con-

secutive 10- μm displacements onto cartilage at a rate of 1 $\mu\text{m}/\text{sec}$. At each step, the displacement was held constant at 10 μm and data were recorded over a period of 300 seconds. The criterion for full relaxation was a change in load of less than 0.005 N over the final 60 seconds. Equilibrium load was measured after each stress relaxation (Fig. 2a).



(a)



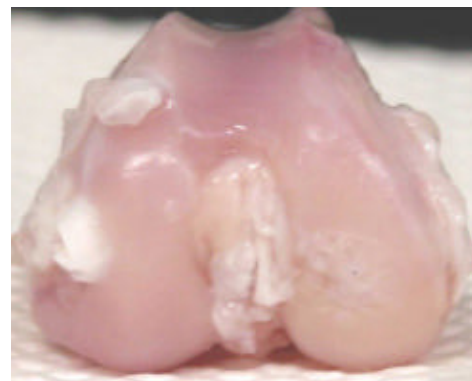
(b)



(c)



(d)



(e)

FIG. 3. (a) Operative view of the defect on the medial femoral condyle (4-mm diameter). (b)–(e) Gross morphology of defects at various intervals. In the control group, the 3-month sample showed small amounts of cartilage-like white tissues appeared at the edge of defect while the PCL scaffold filament is still noticeable (arrow) (b). At 6 months, cartilage-like tissues appeared on the edge while fibrous tissues were in the center of defects (c). In the experimental group, the defect was almost totally repaired with cartilaginous tissues, except for a slight depression in the center 3 months postoperatively, and a good integration appeared between neocartilage and surrounding cartilage (d). At 6 months, the defect was totally repaired by cartilaginous tissues that integrated smoothly with surrounding host tissues (e). (Color images are available online at www.liebertonline.com/ten.)

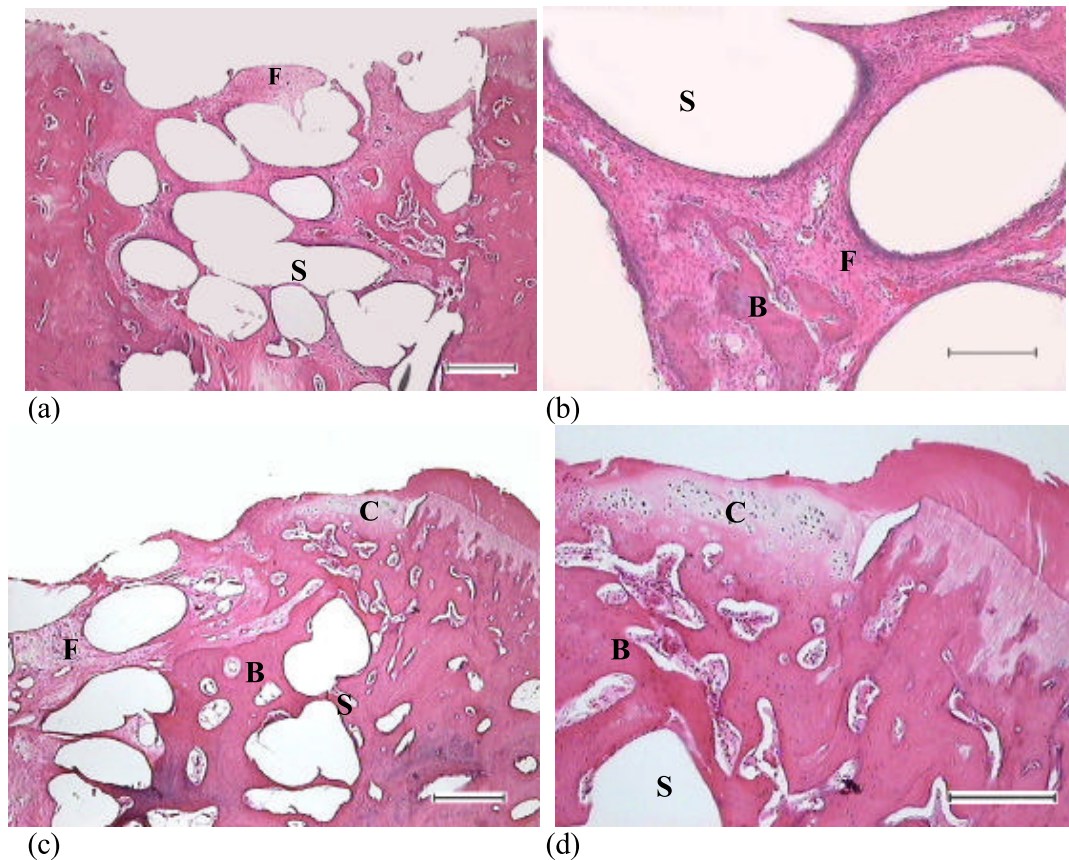


FIG. 4. Histological examination of the control group (HE staining). (a) and (b) Three-month implantation. (c) and (d) Six-month implantation. (a) Fibrous tissues with small bone islands filled in the scaffold and no cartilage formation on the surface. (b) Small bone islands in the fibrous tissues within the scaffolds. Note that the scaffolds have been dissolved in the process of histological preparation and empty spaces were left. (c) At 6 months, more bone tissues and very small portions of cartilage formed. Bone was mixed with the fibrous tissues at the edge of defect and the repair surface was still poor. (d) The cartilage-like tissues appeared adjacent to the native cartilage at the edge of defect. F: fibrous tissues; C: cartilage; B: bone; S: scaffold filament. Bars = 500 μm in (a), (c) and (d); 200 μm in (b). (Color images are available online at www.liebertonline.com/ten.)

After the indentation test, the thickness of the cartilaginous tissue at the test site was determined using a customized needle-probe system. A fine needle was attached to the load cell and stabbed into the cartilage at a constant speed. From the load versus displacement data, the sudden increase in stiffness would indicate that the needle had reached the subchondral bone or implanted scaffolds. The displacement distance of the needle at the instance was taken as the cartilage thickness. This needle-probe system has been verified reliable in normal cartilage thickness detection. The measure results varied from 200 to 400 μm , which were accordant with histology examinations (Fig. 2b).

The Young's modulus, E , of the repaired cartilage was determined using the equation derived from Hayes *et al.*³⁴ for a single phase elastic material:

$$E = P(1 - \nu^2)/2au\kappa$$

where P is the measured load at equilibrium, ν is the Poisson's ratio, a is the radius of the indenter, u is the displacement, κ is the theoretical scaling factor that is dependent on ν , and the ratio a/h_c and h_c is the cartilage thickness at the indentation site.

In the present experiment, Poisson's ratio ν was assumed as 0.2, as previously reported for rabbit medial femoral condyle.³³ Young's moduli were then calculated according to the above equation, using κ value derived from Hayes *et al.*³⁴

Statistical analysis

The control and experimental group were compared with each other and unoperated tissue. Histological scoring data and biomechanical test data were analyzed using one-way analysis of variance test with *post hoc* ($p < 0.05$) from SPSS 10.0 (SPSS Inc., Chicago, IL).

RESULTS

Gross examination

In the control group, without mesenchymal cells, 3-month explants showed a small amount of cartilage-like white tissues at the edge of defect while PCL scaffold filaments were clearly present; 6-month repair samples showed better cartilaginous tissues at the edge and soft fibrous tissue at the center of the defect. In the experimental group, with mesenchymal cells, the defects at 3 months

were almost entirely filled with firm cartilage-like tissues of similar color and texture to the surrounding cartilage. However, in some cases, there was a slight depression in the center of the repair surface. Six-month samples showed a total cartilaginous tissue filling the defects with a relatively smooth surface and good integration (Fig. 3).

Histological analysis

In the control group, 3-month samples showed fibrous tissues formation within the PCL and PCL-TCP scaffolds

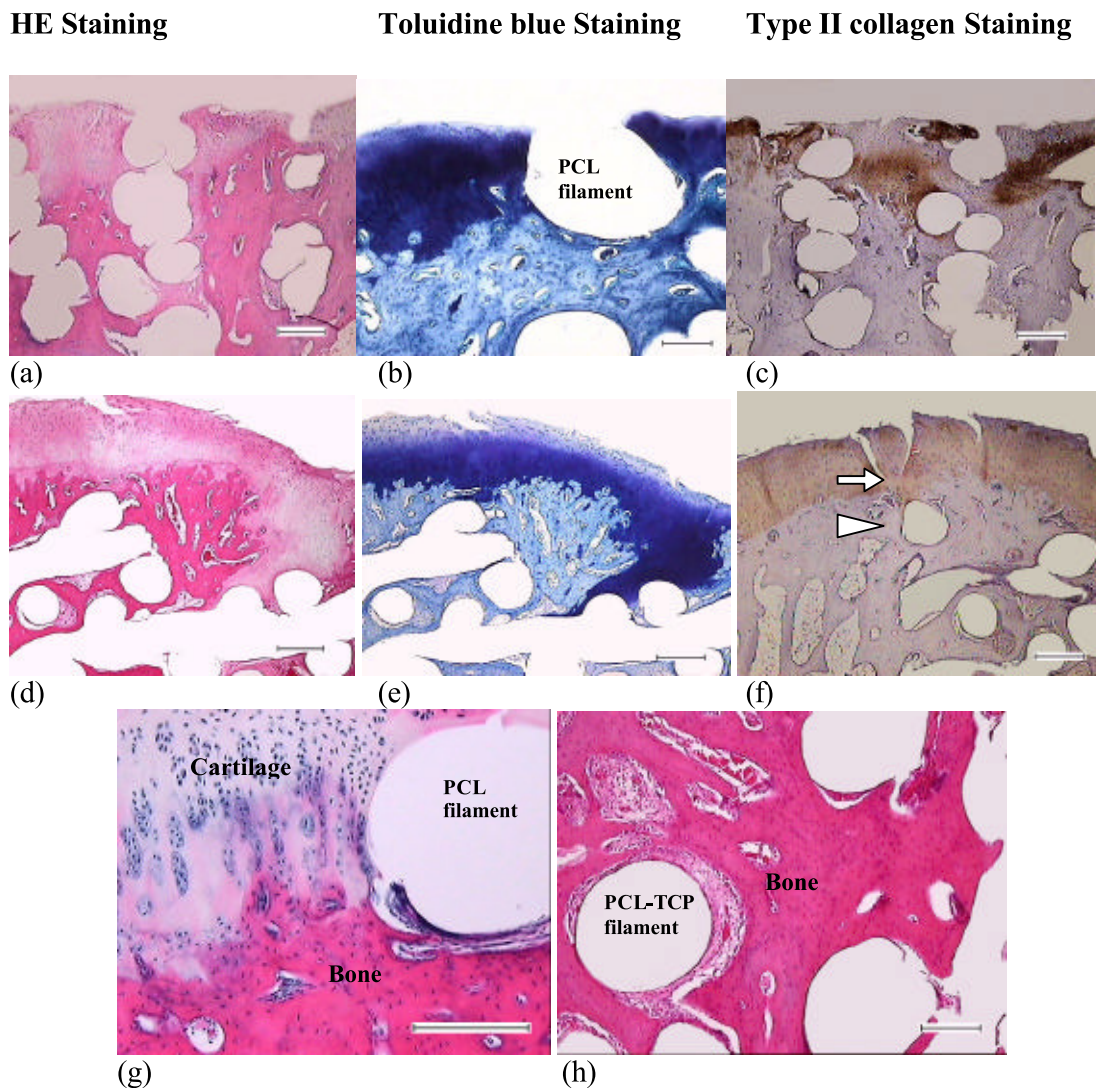


FIG. 5. Histological examination of the experimental group. (a)–(c) After 3 months' implantation, subchondral bone has filled within the PCL-TCP scaffolds; cartilage tissues that expressed specific GAG and Type II collagen mixed with the PCL scaffolds on the surface of defects. (d) and (e) The 6-month sample showed regular subchondral bone filled up in the scaffolds and hyaline-like cartilage layer were formed. The tidemark partially appeared. (f) Some 6-month cases showed fissures at the integration site between new and host cartilage (arrow), whereas bone integrations were well kept (arrowhead). Left: host tissues; Right: regenerated tissues. Type II collagen was expressed through the cartilage layer. (g) Six-month sample: new cartilage formation around the PCL scaffold. (h) Six-month sample: bone formation within the PCL-TCP scaffold. Bars = 500 μm in (a), (c), (d), (e), and (f); 200 μm in (b), (g), and (h). (Color images are available online at www.liebertonline.com/ten.)

TABLE 3. HISTOLOGICAL SCORES OF REPAIR TISSUES, ACCORDING TO TABLE 2^a

Region	Control		Experimental group	
	3 month (n = 3)	6 month (n = 3)	3 month (n = 4)	6 month (n = 5)
Edge of defect	8.3 ± 4.2	10.6 ± 8.0	17 ± 6.6 ^b	23.7 ± 2.0 ^{b-d}
Center of defect	6.3 ± 2.5	9.5 ± 4.8	12.6 ± 2.1 ^b	17.8 ± 2.6 ^b

^aValues are the mean ± SD.

^b $p < 0.05$ versus control group at corresponding time point and area.

^c $p < 0.05$ versus center of defect at 6 month under experimental group.

^d $p < 0.05$ versus 3 month at edge of defect under experimental group.

in the defect. Some small irregular bone islands appeared mixed with the fibrous tissues adjacent to the defect edge. No obvious cartilage-like tissue formed on the surface (Fig. 4a and b). Repaired tissues showed more osteochondral-like characteristics at 6 months postoperatively, although fibrous tissue still dominated over the defect. There were more bone islands in the scaffold around the edge and bottom of defects. Small portions of cartilaginous tissue formed on the site closely adjacent to host cartilage, but the total defect surface was not filled and had no cartilage layer (Fig. 4c and d). The tidemark was not reconstituted.

Compared with the control group, the experimental group showed much better repair in both the bone and cartilage portions. Three months postoperatively, mature trabecular bone could be observed in the PCL-TCP scaffold. Large pieces of cartilage tissue appeared with specific GAG deposition and Type II collagen expression on portions of the defects near the surface. These cartilage tissues mixed with PCL scaffold filaments to form a relative smooth surface over the defect (Fig. 5a–c). Cellular orientation in the neocartilage was disorganized. At 6 months postoperatively, the subchondral bone regularly filled in the scaffold and showed good integration with host bone in all specimens. Cartilage regeneration varied from case to case. Most of the samples showed hyaline-like integrated cartilage layers with even GAG matrix and type II collagen staining. In some cases, fissures and cracks were observed to be present at the integration site between neocartilage and adjacent native cartilage. The cell arrangement in new cartilage was better than 3-month samples but still lacked the typical zonal organization, and a tidemark was partially visible (Fig. 5d–h).

Histological grading scores are presented in Table 3. Overall, within the corresponding time points and locations, the experimental group scored significantly higher than the control group ($p < 0.05$). In the control group, regenerated tissues showed no significant scoring difference between the 3-month and 6-month time points or between the edge and center region of the defect. In the

experimental group, 6-month regenerated tissue at the edge region was better than the 3-month samples (*i.e.*, 23.7 ± 2.0 versus 17 ± 6.6 , $p < 0.05$), whereas central region tissues scores were not significantly different. From the perspective of healing pattern in the defect, 6-month samples from the experimental group showed significantly higher scores at the edge region and lower scores at the central region (*i.e.*, 23.7 ± 2.0 versus 17.8 ± 2.6 , $p < 0.05$), whereas other comparisons between edge and central regions were not significant.

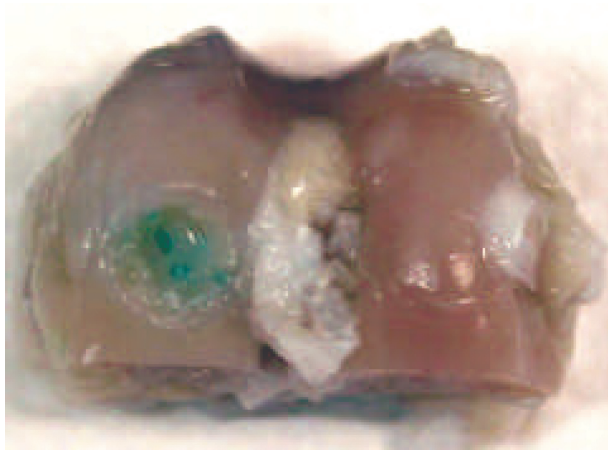
Implanted cell tracing

To investigate the fate of implanted mesenchymal cells in the defect, Adeno-LacZ labeled cells were seeded in both PCL and PCL-TCP scaffolds, and then, implanted *in vivo*. In the 6-week repaired samples, blue color tissues filled within the scaffolds after X-gal staining (Fig. 6a and b). Histological sections from coronal plane with Safranin-O counterstaining also showed the presence of implanted cells in the defect. These blue cells stayed in the fibrous tissues around the scaffold filaments (Fig. 6c).

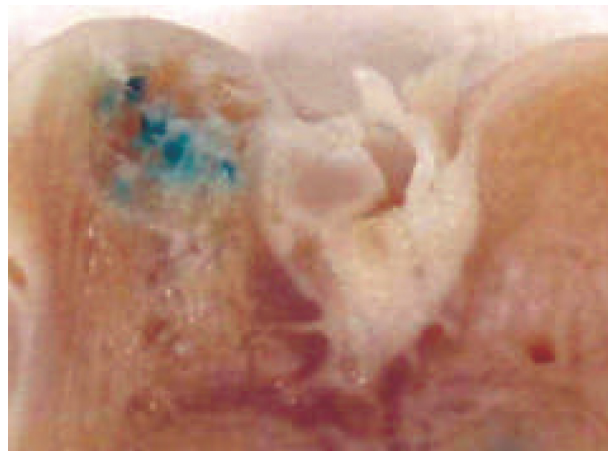
Biomechanical findings

From the indentation test, the Young's moduli of repaired tissues from control and experimental groups were determined and compared with each other while the tissues from unoperated rabbit medial femoral were used as normal control (Fig. 7). At all time points, the stiffness of experimental group samples showed greater improvement as compared with specimens from the control group ($p < 0.05$). At 3 months postoperatively, samples from both control and experimental group had inferior stiffness values to normal unoperated cartilage ($p < 0.05$). At 6 months postoperatively, there was no significant difference between experimental group samples and normal unoperated cartilage. This indicates that after 6-month implantation, the stiffness of repaired tissues in the experimental group was similar to that of the normal cartilage.

a



b



c

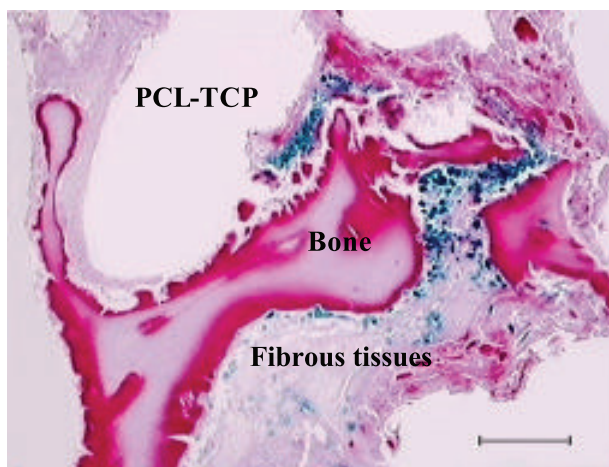


FIG. 6. X-gal staining for implanted cells tracing. (a) Blue color tissues filled within the scaffolds. (b) After decalcification, a coronal section showed blue tissues in the defect. (c) Histological section showed the blue color tissues in the defect. Safranin-O counterstaining; bar = 200 μm . (Color images were available online at www.liebertonline.com/ten.)

DISCUSSION

Many research groups had investigated the potential of osteochondral repair in defects of rabbit femoral patellar groove by using different types of polymeric scaffolds with chondrocytes.^{4,35,36} Most of the authors reported achieving good results; however, these defect models did not reflect the frequently encountered clinical problem, *i.e.*, defects at sites of high biomechanical loading. Athanasiou *et al.* reported that the patellar groove had the lowest aggregate modulus of different regions on the distal femur.³⁷ It should be noted that the articular cartilage of rabbits and dogs in the low load-bearing areas are thinner than those in high weight-bearing areas. So, in the current study, the defects were designed at the weight-bearing site to simulate the targeted clinical situation as closely as possible. It is well known that a large full-thickness cartilage defect ($\geq 3\text{-mm}$ diameter) in mature rabbit models would not heal spontaneously.^{38,42} Thus, a critical-sized defect (4-mm diameter \times 5.5-mm depth) affecting more than 50% of the surface area was created on the medial femoral condyle, following the hybrid scaffolds implantation with or without BMSC, whereas the empty defects (without treatment) were not included in our experimental design.

Articular osteochondral defect repair involves two types of distinct tissues: articular cartilage and subchondral bone. Developing hybrid or biphasic scaffolds for osteochondral defects has been gaining popularity in the field of tissue engineering. Hung *et al.* reported using an agarose gel loaded with chondrocytes on a bovine tra-

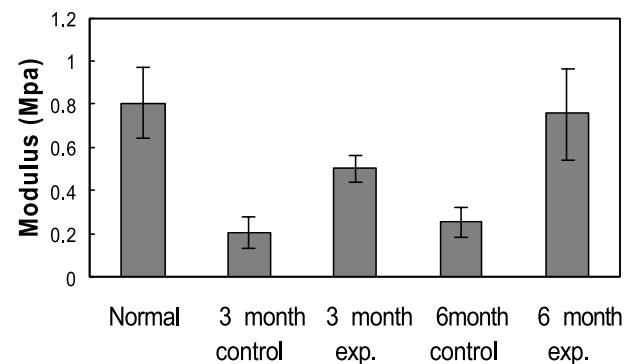


FIG. 7. Biomechanical analysis of the repair tissues. Values represent mean and standard deviation ($n = 6$ in normal group, $n = 3$ in 3-month control, $n = 5$ in 3-month exp. $N = 5$ in 6-month control, $n = 6$ in 6-month exp.). At all time points, there was statistical significance between the experimental and control group ($p < 0.05$). At 3 months, modulus from either the control or experimental group was significantly inferior to the normal cartilage ($p < 0.05$). At 6 months, modulus of the control group was significantly lower than that of the normal cartilage ($p < 0.05$), whereas experimental group samples were similar to the normal cartilage.

becular bone block to generate an osteochondral construct *in vitro*.³⁹ A biphasic osteochondral scaffold from Schaefer *et al.* was created by suturing a subchondral bone support, *i.e.*, collagraft with pre-engineered cartilage that was generated *in vitro* from chondrocytes on PGA mesh.³⁴ Implantation of this composite in rabbit patellar groove defects achieved good osteochondral reconstruction. However, 4 to 6 weeks of *in vitro* culture for engineered cartilage is time-consuming work and may not be convenient for further clinical application. A very recent report showed a bi-phased scaffolds system made of chondrocytes in collagen gel overlying porous tricalcium phosphate blocks that were grafted into rabbit femoral patellar groove defects.⁴⁰ Hyaline-like cartilage was dominant up to 12 weeks' implantation but degenerated at 30 weeks, whereas 76% of repair tissues were fibrocartilage and fibrous tissues at that time. One of reasons for the cartilage deterioration was due to biomechanical incompatibility occurring at the junction site, *i.e.*, the lower stiffness of collagen gel and tricalcium phosphate and their fast degradation rates.

In the present study, PCL scaffold with a slow degradation rate was used for the cartilage portion, while PCL-TCP scaffold was used for the bony portion. The results demonstrated that hybrid scaffolds seeded with BMSCs could promote the repair of critical-sized osteochondral defects in high load-bearing sites after 6 months' implantation. The regenerated tissues showed good subchondral bone formation, a hyaline-like cartilage surface, and restoration of biomechanical stiffness, although cellular arrangement in the new cartilage lacked the typical zonal characteristics, and some fissures appeared in some samples. In contrast, the control group showed very limited osteochondral regeneration.

Chu *et al.* reported a study on osteochondral defect repair by perichondrocytes seeded on a poly lactic acid mesh at 12-week, 6-month, and 1-year follow-up.⁴¹ In their experiments, it was found that the subchondral bone reformation was inconsistent, only reaching 50% at 1-year follow-up. The neocartilage also deteriorated with time; the region of ideal repair occupied by hyaline cartilage decreased from 95% at 12 weeks to 65% at 6 months and only 29% at 1-year follow-up. The authors attributed this inconsistent restoration to host immune reaction to the allograft. However, other important factors might be present, *i.e.*, insufficient mechanical support of the neocartilage or subchondral bone because of the lower mechanical strength of PLA scaffold, and a faster degradation rate (The author showed their single PLA scaffold, under normal physiological loading, appeared to degrade during a 12-week period). Qiu *et al.*⁴² reported a study of spontaneous subchondral bone formation during osteochondral repair without any treatment. After 16 weeks, the repaired surface nonosseous layer became thinner and showed disappearance of safranin-O staining,

increased separation splits at the boundary, and eventual degradation. The authors believed the presence of an irregular subchondral bone was associated with degradation of the repaired articular surface. Abnormal subchondral bone is one of the major factors in influencing the long-term outcome of articular cartilage repair.

Therefore, in articular osteochondral reconstruction, ideal 3D scaffolds should provide sufficient strength over a long enough period of time to withstand *in vivo* physiological forces. Our previous studies had shown that the PCL scaffold had a compressive stiffness 29.4 ± 4.0 MPa in simulated physiological conditions and would begin to lose mechanical properties gradually over 9 to 12 months, until it is completely metabolized by 2 years.^{11,17} In the current study, the hybrid scaffolds still existed in defects and offered mechanical support at 6 months postoperatively. This scaffold complex was highly biocompatible and matched well with the regenerated subchondral bone and cartilage, which was demonstrated by histology analysis. Meanwhile, from the functional biomechanical test, the stiffness of the tested area revealed the overall strength of neo-tissue-polymer matrix. The area under compression was only the materials under the indenter, which were only the newly regenerated tissue and scaffold polymers. The mechanical test results showed that the cell-seeded scaffolds have comparable strength to the normal cartilage at 6 months. The slower degradation of the PCL-based hybrid scaffolds may leave remnants in the repair space over a longer time. However, it is these remnants that help maintain enough mechanical support for the subchondral bone and neocartilage. A weakness in the current study was the shorter experimental time and smaller sample numbers. A 9- or 12-month postoperative time point should be included to address the change of scaffolds and repair tissues.

Many previous studies have reported that bone marrow mesenchymal cells combined with scaffold implantation can promote osteochondral repair.^{1,5,10,11,27,28} This is further demonstrated in the current study. Compared with cell-free scaffold transplantation, addition of mesenchymal cells showed significant improvement in both bone and cartilage regeneration. The *in vivo* tracing experiment confirmed that these transplanted foreign cells can survive for at least 6 weeks after implantation. This indicated that the allogeneic mesenchymal cells could survive and participate in further regeneration of bone and cartilage. An interesting point was that these transplanted cells did not show up in the new osteochondral tissues but only resided within the fibrous tissues around the scaffolds filaments, which meant the implanted cells did not form into new bone or cartilage. This phenomenon did reveal some clues for the fate of implanted cells, although a 6-week period was not long enough.

One recent article reported the fate of perichondrium cells in osteochondral defects after transplantation with

PLA in rabbits.⁴³ Donor cells were present in repair tissue for 28 days after implantation. However, the number of donor cells declined from approximately 1 million at day zero to approximately 140,000 after 28 days. This decline in donor cells was accompanied by a significant influx of host cells into the repair tissue. Indirectly, our histological score data from the experimental group also showed similar results. The edges of defects were scored higher than the central zone after 6 months; the scores at the edge region showed an increase from 3 months to 6 months while there was no difference in the central region. Overall, it is quite possible that host cells still dominate in the repair process while the implanted cells serve as tissue templates by secreting cellular matrix or bioactive factors that promote new tissue formation or recruit host cells migration, and are finally replaced by the host cells. Currently, little is known of fate of the implanted mesenchymal cells *in vivo* and how the cells influence new tissue repair, although these cells have been extensively used as promising candidates for cell therapy in the field of tissue engineering. The tracing experiment in our study was not quantitative and the time period was short. These limitations should be resolved in further investigations.

From this study, it has been shown that the BMSCs-seeded PCL and PCL-TCP hybrid scaffold system might be an alternative approach for osteochondral defect repair. The current findings warrant further investigation with longer track time so as to draw a clearer map of the PCL-based hybrid scaffolds. Optimization of the scaffold system, such as fabrication of real integrated biphasic materials with reduced thickness of the cartilage region, and extension to a large animal model will be other directions of investigation.

ACKNOWLEDGMENTS

This work was supported by Singapore National Medical Research Council grants #NMRC/0444/2000. We would like to thank Ms. Chong Sue Wee for her kindly technical assistance.

REFERENCES

- Grande, D.A., Breitbart, A.S., Mason, J., Paulino, C., Laser, J., and Schwarz, R.E. Cartilage tissue engineering: current limitations and solutions. *Clin. Orthop.* **367s**, 176, 1999.
- Hunziker, E.B. Biological repair of articular cartilage-defect models in experimental animals and matrix requirements. *Clin. Orthop. Rel. Res.* **367s**, 135, 1999.
- Boyan, B.D., Lohmann, C.H., Romero, J., and Schwartz, Z. Bone and cartilage tissue engineering. *Clin. Plast. Surg.* **26**, 629, 1999.
- Wakitani, S., Goto, T., Young, R.G., Mansour, J.M., Goldberg, V.M., and Caplan, A.I. Repair of large full-thickness articular cartilage defects with allograft articular chondrocytes embedded in a collagen gel. *Tissue Eng.* **4**, 429, 1998.
- Wakitani, S., Goto, T., Pineda, S.J., Young, R.G., Mansour, J.M., Caplan, A.I., and Goldberg, V.M. Mesenchymal cell-based repair of large, full-thickness defects of articular cartilage. *J. Bone Joint Surg. Am.* **76**, 579, 1994.
- Douchis, J.S., Coutts, R.D., and Amiel, D. Cartilage repair with autogenic perichondrium cell/poly(lactic acid) grafts: a two-year study in rabbits. *J. Orthop. Res.* **18**, 512, 2000.
- Caplan, A.I., and Goldberg, V.M. Principles of tissue engineered regeneration of skeletal tissues. *Clin. Orthop.* **367s**, 12, 1999.
- Caplan, A.I. Tissue engineering designs for the future: new logics, old molecules. *Tissue Eng.* **6**, 1, 2000.
- Ben-yishay, A., Grande, D.A., Menche, D., Pitman, M.D., and Schwarz, R.E. Repair of articular cartilage defects with collagen-chondrocyte allografts. *Tissue Eng.* **2**, 119, 1995.
- Diduch, D.R., Jordan, L.C., Mierisch, C.M., et al. Marrow stromal cells embedded in alginate for repair of osteochondral defects. *Arthroscopy* **16**, 571, 2000.
- Hutmacher, D.W. Scaffolds in tissue engineering bone and cartilage. *Biomaterials* **21**, 2529, 2000.
- Gao, J., Dennis, J.E., Solchaga, L.A., Awadallah, A.S., Goldberg, V.M., and Caplan, A.I. Tissue-engineered fabrication of an osteochondral composite graft using rat bone marrow-derived mesenchymal stem cells. *Tissue Eng.* **7**, 363, 2001.
- Frenkel, S.R., Toolan, B., Menche, D., Pitman, M.I., and Pachence, J.M. Chondrocyte transplantation using a collagen bilayer matrix for cartilage repair. *J. Bone Joint Surg. Br.* **79**, 831, 1997.
- van Susante, J.L., Buma, P., Homminga, G.N., van den Berg, W.B., and Veth, R.P. Chondrocyte-seeded hydroxyapatite for repair of large articular cartilage defects. A pilot study in the goat. *Biomaterials* **19**, 2367, 1998.
- Zein, I., Hutmacher, D.W., Tan, K.C., and Teoh, S.H. Fused deposition modeling of novel scaffold architectures for tissue engineering applications. *Biomaterials* **23**, 1169, 2002.
- Deshpande, A.A., Heller, J., and Gurny, R. Bioerodible polymers for ocular drug delivery. *Crit. Rev. Ther. Drug Carrier Syst.* **15**, 381, 1998.
- Hutmacher, D.W., Schantz, T., Zein, I., Ng, K.W., Teoh, S.H., and Tan, K.C. Mechanical properties and cell cultural response of polycaprolactone scaffolds designed and fabricated via fused deposition modeling. *J. Biomed. Mater. Res.* **55**, 203, 2001.
- Huang, Q., Goh, J.C., Hutmacher, D.W., and Lee, E.H. In vivo mesenchymal cell recruitment by a scaffold loaded with transforming growth factor beta1 and the potential for in situ chondrogenesis. *Tissue Eng.* **8**, 469, 2002.
- LeGeros, R.Z. Properties of osteoconductive biomaterials: calcium phosphates. *Clin. Orthop.* **395**, 81, 2002.
- Oreffo, R.O., and Triffitt, J.T. Future potentials for using osteogenic stem cells and biomaterials in orthopedics. *Bone* **25**, 5S, 1995.
- Bucholz, R.W. Nonallograft osteoconductive bone graft substitutes. *Clin. Orthop.* **395**, 44, 2002.
- Peter, S.J., Miller, M.J., Yasko, A.W., Yaszemski, M.J.,

- and Mikos, A.G. Polymer concepts in tissue engineering. *J. Biomed. Mater. Res.* **43**, 422, 1998.
23. Schantz, J.T., Hutmacher, D.W., Lam, C.X., Brinkmann, M., Wong, K.M., Lim, T.C., Chou, N., Guldberg, R.E., and Teoh, S.H. Repair of calvarial defects with customised tissue-engineered bone grafts II. Evaluation of cellular efficiency and efficacy in vivo. *Tissue Eng.* **9** Suppl, 127, 2003.
 24. Yoo, J.U., Brun, P., Cortivo, R., Schaga, L., Caplan, A.I., et al. The chondrogenic potential of human bone marrow-derived mesenchymal progenitor cells. *J. Bone Joint Surg. Am.* **80A**, 1745, 1998.
 25. Cassiede, P., Dennis, J.E., Ma, F., and Caplan, A.I. Osteochondrogenic potential of marrow mesenchymal progenitor cells exposed to TGF- β 1 or PDGF-BB as assayed in vivo and in vitro. *J. Bone Miner. Res.* **11**, 1264, 1996.
 26. Pittenger, M.F., Mackay, A.M., Beck, S.C., Jaiswal, R.K., and Douglas, R., et al. Multilineage potential of adult human mesenchymal stem cells. *Science* **284**, 143, 1999.
 27. Im, G.I., Kim, D.Y., Shin, J.H., Hyum, C.W., et al. Repair of cartilage defect in the rabbit with cultured mesenchymal stem cells from bone marrow. *J. Bone Joint Surg.* **83B**, 289, 2001.
 28. Butnariu-Ephrat, M., Robinson, D., Mendes, D.G., Halperin, N., and Nevo, Z. Resurfacing of goat articular cartilage by chondrocytes derived from bone marrow. *Clin. Orthop.* **330**, 234, 1996.
 29. Goshima, J., Goldberg, V.M., and Caplan, A.I. The osteogenic potential of culture-expanded rat marrow mesenchymal cells assayed in vivo in calcium phosphate ceramic blocks. *Clin. Orthop.* **262**, 298, 1991.
 30. Gundle, R., Joyner, C.J., and Triffitt, J.T. Human bone tissue formation in diffusion chamber culture in vivo by bone-derived cells and marrow stromal fibroblastic cells. *Bone* **16**, 597, 1995.
 31. Kadiyala, S., Young, R.G., Thiede, M.A., and Bruder, S.P. Culture expanded canine mesenchymal stem cells possess osteochondrogenic potential in vivo and in vitro. *Cell Transplant.* **6**, 125, 1997.
 32. Solchaga, L.A., Yoo, J.U., Lundberg, M., Dennis, J.E., Huibregtse, B.A., Goldberg, V.M., and Caplan, A.I. Hyaluronan-based polymers in the treatment of osteochondral defects. *J. Orthop. Res.* **18**, 773, 2000.
 33. Hayes, W.C., Keer, L.M., Herrmann, G., and Mockros, L.F.A. Mathematical analysis for indentation tests of articular cartilage. *J. Biomech.* **5**, 541, 1972.
 34. Schaefer, D., Martin, I., Jundt, G., Seidel, J., Heberer, M., Grodzinsky, A., Bergin, I., Vunjak-Novakovic, G., and Freed, L.E. Tissue-engineered composites for the repair of large osteochondral defects. *Arthritis Rheum.* **46**, 2524, 2002.
 35. Schreiber, R.E., Ilten-Kirby, B.M., Dunkelmann, N.S., Symons, K.T., Rekettye, L.M., Willoughby, J., and Ratcliffe, A. Repair of osteochondral defects with allogeneic tissue engineered cartilage implants. *Clin. Orthop.* **367s**, 382, 1999.
 36. Mainil-Varlet, P., Rieser, F., Grogan, S., Mueller, W., Saager, C., and Jakob, R.P. Articular cartilage repair using a tissue-engineered cartilage-like implant: an animal study. *Osteoarthritis Cartilage* **9s**, 6, 2001.
 37. Athanasiou, K.A., Rosenwasser, M.P., Buckwalter, J.A., Malinin, T.I., and Mow, V.C. Interspecies comparisons of in situ intrinsic mechanical properties of distal femoral cartilage. *J. Orthop. Res.* **9**, 330, 1991.
 38. Shapiro, F., Koide, S., and Glimcher, M.J. Cell origin and differentiation in the repair of full-thickness defects of articular cartilage. *J. Bone Joint Surg. Am.* **75**, 532, 1993.
 39. Hung, C.T., Lima, E.G., Mauck, R.L., Taki, E., LeRoux, M.A., Lu, H.H., Stark, R.G., Guo, X.E., and Ateshian, G.A. Anatomically shaped osteochondral constructs for articular cartilage repair. *J. Biomech.* **36**, 1853, 2003.
 40. Tanaka, T., Komaki, H., Chazono, M., and Fujii, K. Use of a biphasic graft constructed with chondrocytes overlying a beta-tricalcium phosphate block in the treatment of rabbit osteochondral defects. *Tissue Eng.* **11**, 331, 2005.
 41. Chu, C.R., Douchis, J.S., Yoshioka, M., Sah, R.L., Coutts, R.D., and Amiel, D. Osteochondral repair using perichondrial cells. A 1-year study in rabbits. *Clin. Orthop.* **340**, 220, 1997.
 42. Qiu, Y.S., Shahgaldi, B.F., Revell, W.J., and Heatley, F.W. Observations of subchondral plate advancement during osteochondral repair: a histomorphometric and mechanical study in the rabbit femoral condyle. *Osteoarthritis Cartilage.* **11**, 810, 2003.
 43. Ostrander, R.V., Goomer, R.S., Tontz, W.L., Khatod, M., Harwood, F.L., Maris, T.M., and Amiel, D. Donor cell fate in tissue engineering for articular cartilage repair. *Clin. Orthop.* **389**, 228, 2001.

Address reprint requests to:

James C.H. Goh, Ph.D.

Department of Orthopaedic Surgery

National University of Singapore

10 Lower Kent Ridge Road

Singapore 119260

E-mail: dosgohj@nus.edu.sg

